Supporting Information

Moon et al. 10.1073/pnas.1006646107

SI Materials and Methods

Cell Lines and Cell Culture. The mouse mammary carcinoma cell line 4T1 was maintained in RPMI-1640. The human breast cancer cell line MDA-MB-231 was grown in MEM, and the human cervix cancer cell line SiHa was cultured in DMEM. All cell lines were obtained from the America Type Culture Collection (ATCC). All media were supplemented with 10% FBS and 100 units/mL penicillin/streptomycin. Cells were maintained in a 37 °C incubator with 5% CO_2.

Hyperthermia Treatment in Vitro. Cells (2×10^6) were seeded in T25 flasks and grown overnight. Flasks were tightly sealed with parafilm, and the bottom was submerged in a preheated water bath and treated for 1 h. Immediately after treatment or after incubation for 6 or 24 h at 37 °C, cells were lysed and protein or RNA was extracted.

Western Blot. Immediately or 6 and 24 h after treatment, whole-cell protein was extracted by adding a Radio-Immunoprecipitation (RIPA) lysis buffer (Pierce) with 1× protease inhibitor (Thermo Scientific). Fifty micrograms of protein was separated on 4–15% Tris·HCl gels (BioRad) and transferred to a 0.2-μM Immun-Blot PVDF membrane (Bio-Rad). The membrane was blotted using the following antibodies: HIF-1α (Novus Biologicals), phospho-ERK1/2 (Cell Signaling), ERK1/2 (Millipore), phospho-p38 (Cell Signaling), p-38 (Cell Signaling), phospho-JNK (Cell Signaling), JNK (Santa Cruz Biotechnology), and β-actin (Sigma). Experiments were repeated at least three times.

Clonogenic Assays. Effect of HT on tumor cell survival was determined using clonogenic assay. One hundred 4T1 cells were seeded into each well of a six-well plate. Cells were incubated with 2.5 mL of cell medium for 24 h and HT-treated for 1 h. After HT treatment, cell medium was removed and cells were washed with PBS. In each well, fresh medium was added and cells were incubated for 1 wk until colonies were visible. After brief washing with PBS, colonies were fixed with fixation solution (10% methanol, 10% acetic acid, 80% H_2O) for 10 min and stained with 0.4% crystal violet (200 ml of 4% crystal violet, 200 ml of H_2O, and 100 ml of ethanol). Colonies containing more than 50 cells were counted. The number of colonies at each treatment group was normalized to 37 °C.

Quantitative Real-Time Reverse Transcriptase PCR. Total mRNA was extracted using a miRVana extraction kit (Ambion). One microgram of mRNA was reverse-transcribed into cDNA using an iScript cDNA synthesis kit (BioRad). Quantitative real-time RT-PCR was performed with Power SYBRGreen PCR Mix (Applied Biosystems) using the ABI 7900HT Fast Real-Time PCR System (Applied Biosystems). Each primer sequence is indicated in Table S1. The expression level of each mRNA was normalized to β-actin expression in the same sample. Experiments were repeated at least three times.

siRNA Transfection. Cells were seeded into six-well plates and grown overnight. Cells were transfected with SMARTpool siRNA (Dharmacon) against human HIF-1α, NOX1, cytochrome C, or nontargeting control using lipofectamine RNAiMAX (Invitrogen) according to the manufacturer's protocol. mRNA and protein expression of knockdown cells were determined 48 h after transfection and were compared with cells transfected with control siRNA, a nontargeting POOL (Dharmacon).

Lactate Measurement. When tumor tissues were excised, mouse blood was collected using a heparin-coated syringe. Blood was transferred into a heparin-coated microcentrifuge tube and spun at $300 \times g$ for 30 min. Plasma, which remained as a supernatant, was collected and stored at −80 °C (until analysis. Lactate levels in mouse plasma were analyzed using an EnzyChrom L-Lactate Assay Kit (BioAssay).

HIF-1 ELISA. Immediately after 1 h of HT, nuclear proteins were extracted from 4T1 cells using a NucBuster Protein protein extraction kit (Novagen). Mouse tumor tissues, which were collected 6, 24, and 48 h after treatment, were homogenized, and tissue protein was collected by adding lysis buffer (Pierce) with 1× proteinase inhibitor (Thermo Scientific). Ten micrograms of nuclear or total protein was added into a 96-well plate in triplicate, and hypoxia response element-bound HIF-1α levels were measured using a Human/Mouse Active HIF-1a Activity Assay ELISA kit (R&D Systems and Active Motif) following the manufacturers' protocols. Experiments were repeated at least three times.

Vascular Endothelial Growth Factor ELISA. Immediately after or 6 and 24 h after HT, 4T1 cell culture medium was collected. After briefly spinning down cell culture media for 10 min at $15{,}800 \times g$, 50 μL of supernatant was added into a 96-well plate provided in a mouse Quantikine VEGF ELISA kit (R&D Systems). For in vivo measurements, 20 μg of total protein extracted from tumor tissues was added into a 96-well plate from the same kit. Vascular endothelial growth factor (VEGF) levels were quantified following the manufacturer's protocol. Experiments were repeated at least three times.

Animal Studies. 4T1-ODD-Luc cells (5×10^5) in 100 μL of PBS were subcutaneously injected into the right flank of female nude mice. When tumor size reached 200 mm^3, mice were randomized into two groups: control and HT ($n = 8$). Mice were anesthetized and placed in a Plexiglas mouse holder designed to allow the tumor-bearing legs to be submerged into the HT water bath for 1 h. To protect the skin from water and prevent edema, the tumor-bearing portion of the leg was wrapped with a plastic bag, and the mouse leg was then submerged into the prewarmed water bath heated to a temperature of 43.5 °C. Tumor core temperatures reached 42–43 °C. During treatment, body temperature remained unchanged from baseline (data not shown). Mice in the control group were treated using a water bath heated to 34 °C, a temperature that corresponds to mouse skin temperature.

In Vivo Bioluminescence Imaging. At various time points after HT, ODD-luciferase signals in mouse tumors were detected and quantified as previously described (12). Briefly, at various time points (0, 3, 6, 12, 24, 48, and 72 h) after treatment, mice were anesthetized by inhaling isoflurane. During anesthesia, mice were given an i.p. injection of luciferin (150 mg/kg), and 20 min later they were noninvasively imaged using the Xenogen IVIS bioluminescence imaging system (Xenogen Corporation) (12). The luciferase signal was analyzed with the Living Image Software (Xenogen Corporation).

Immunohistochemistry. Tumor tissues were surgically removed from five mice in each treatment group (HT vs. control) at various time points (6, 24, and 48 h) after treatment. Before excising the tumors, the hypoxia marker EF5 (100 μM/L i.p., obtained from Cameron Koch, University of Pennsylvania, Philadelphia) and

the perfusion marker Hoechst 33342 (1 mg/kg i.v., Sigma-Aldrich) were injected as previously described (2). Once removed, tumors were snap-frozen in liquid nitrogen and stored at −80 °C until analysis.

For fluorescent imaging, 10-μm tumor sections were cut using a cryomicrotome. With modifications to what was previously described (2), EF5 and CD31 were imaged on the same tissue section. Briefly, air-dried tissue sections were fixed in 100% methanol for 30 min and washed twice with PBS. After blocking with 5% donkey serum for 1 h, tissue sections were incubated with anti-mouse CD31 antibody (1:100 dilution; BD Pharmingen) and Cy3-labeled anti-EF5 antibody (ELK3-51, 1:2 dilution, obtained from Cameron Koch) overnight at 4 °C in the dark. After washing three times with PBS, tissue sections were incubated with Alexa Fluor 488-conjugated secondary antibody (1:1,000 dilution; Invitrogen) for 1 h at room temperature. Following three additional washing steps with PBS, slides were stored in 1% paraformaldehyde at 4 °C until they were imaged. Images were taken following previously reported procedures (2–4) using a fluorescence microscope (Axioskop 2 plus, Zeiss). A TRITC fluorescence filter was used for Cy3-EF5 imaging and a FITC fluorescence filter was used for CD31 imaging. Hoechst 33342 was imaged using a DAPI filter. Images were acquired from stage scanning and stitched using MetaMorph Imaging Software (Molecular Devices).

VEGF was stained following the previous protocol (4). Briefly, 10-μm tumor sections were air-dried for 30 min and fixed for 10 min in cold acetone. Tissues were air-dried again for 30 min and incubated with PBS for 5 min. After 30 min of blocking with 10% donkey serum, tissues were incubated overnight at 4 °C with VEGF antibody (1:500 dilution; Santa Cruz Biotechnology). Slides were washed three times in PBS for 5 min followed by incubation with the secondary antibody (Jackson ImmunoResearch) for 30 min at room temperature. Again slides were washed three times in PBS for 5 min followed by incubation with ABC-Elite (Vector Laboratories) for 30 min at room temperature. Reaction was localized by using 3.3′-diaminobenzidine tetrachloride working solution (Lab Vision). Finally, the slides were counterstained with Harris hematoxylin (Fisher Scientific) and mounted with coverslips. For image analysis, the slides were systematically scanned with a light microscope (Zeiss Axioskop 2 plus) and digital images were acquired from each slide with 20× objectives using the Axiovision 3.1 software.

For bioluminescence imaging, tissue was cut into 20-μm sections. After freeze-drying tissue sections using a lyophilizer, ATP images were taken as previously described (2).

Image Analysis. Regions of interest (ROIs) were drawn around the viable tumor area using ImageJ Software. Percentage of tumor perfused areas was calculated by measuring Hoechst 33342-positive areas divided by the whole viable tumor area. Blood vessel number was counted after adjusting the threshold of CD31-positive areas. The number of vessels was counted in both whole viable areas and perfused areas, and the percentage of blood vessels in perfused areas was calculated. Hypoxic tumor area was obtained as previously described (3). Briefly, ROIs were drawn around the viable tumor area, and images were thresholded using the Otsu thresholding method built in ImageJ Software. Hypoxic areas were determined by calculating the percentages of EF5-positive areas.

EPR Oximetry. Changes in oxygen consumption rate were measured using 4T1 cells as previously described (5). Briefly, after HT treatment, 2×10^7 4T1 cells/mL were sealed in glass capillary tubes in the presence of 0.2 mM of the O_2 sensor 4-oxo-2,2,6,6-tetramethylpiperidine-D-^{15}N-1-oxyl (CDN isotopes). Cells were maintained at 37 °C during recording on a Bruker EMX EPR spectrometer operating at 9 GHz.

PDK1 shRNA. pLKO 0.1 lentiviral vectors expressing scramble (Addgene) and PDK1 shRNA (clone TRCN0000078809; Sigma) were used to generate viral particles with the lentiviral packaging mix (Sigma) according to the manufacturer's instructions. Briefly, HEK293FT cells were transiently transfected with lipofectamine using a third-generation lentiviral system; after 24 and 48 h, viral supernatant was harvested, titrated, and used to infect 4T1 cells. Puromycin selection (1 μg/mL) was applied after lentiviral infection.

ROS Measurements. After HT, cells were washed with PBS and collected by scraping. Cells (1×10^6) were counted and incubated with 5 μM of 5-(and-6)-chloromethyl-2′,7′-dichlorodihydrofluorescein diacetate, acetyl ester (CM-H_2DCFDA; Invitrogen) at 37 °C with 5% CO_2 in the dark. After 30 min, cells were briefly washed with PBS, and the intensity of DCFDA was measured by flow cytometry.

Mitochondrial Membrane Potential Measurement. Mitochondrial membrane potential was measured using a MitoProbe JC-1 Assay Kit (Invitrogen). Briefly, cells were HT-treated for 1 h and washed with PBS. Cells were counted and 10^6 cells/mL were incubated with 2 μM of JC-1 for 30 min at 37 °C with 5% CO2 in the dark. Cells were washed with PBS and analyzed by flow cytometry using 488 nm excitation and green (monomer) and red (aggregates) emission. Red -to to-green ratio was evaluated to assess changes in mitochondrial membrane potential.

NADP+/NADPH Rratio. HT-treated MDA-MB-231 cells were washed with PBS, scraped, and collected. After centrifugation, 106 cells were resuspended in the NADP+/NADPH extraction buffer included in the NADP+/NADPH quantification kit (Biovision). The $NADP^+$/NADPH ratio was determined following the manufacturer's protocol.

In Vitro ATP Assay. After HT, 4T1 cells were washed with PBS and collected by scraping. Cells (2×10^4) were transferred into each well of a 96-well plate. ATP was measured using a CellTiter-Glo Luminescent Cell Viability Assay kit (Promega).

Statistical Analysis. Student's *t* test or one- or two-way ANOVAs with posthoc Fisher's protected least significant difference (PLSD) tests were performed to determine statistical significance. All error bars represent the mean ± SD or mean ± SEM.

1. Li F, et al. (2007) Regulation of HIF-1alpha stability through S-nitrosylation. *Mol Cell* 26: 63–74.
2. Schroeder T, et al. (2005) Spatial heterogeneity and oxygen dependence of glucose consumption in R3230Ac and fibrosarcomas of the Fischer 344 rat. *Cancer Res* 65: 5163–5171.
3. Yuan H, et al. (2006) Intertumoral differences in hypoxia selectivity of the PET imaging agent 64Cu(II)-diacetyl-bis(N4-methylthiosemicarbazone). *J Nucl Med* 47:989–998.
4. Rabbani ZN, et al. (2009) Antiangiogenic action of redox-modulating Mn(III) meso-tetrakis(N-ethylpyridinium-2-yl)porphyrin, MnTE-2-PyP(5+), via suppression of oxidative stress in a mouse model of breast tumor. *Free Radic Biol Med* 47:992–1004.
5. Jordan BF, et al. (2003) Nitric oxide-mediated increase in tumor blood flow and oxygenation of tumors implanted in muscles stimulated by electric pulses. *Int J Radiat Oncol Biol Phys* 55:1066–1073.

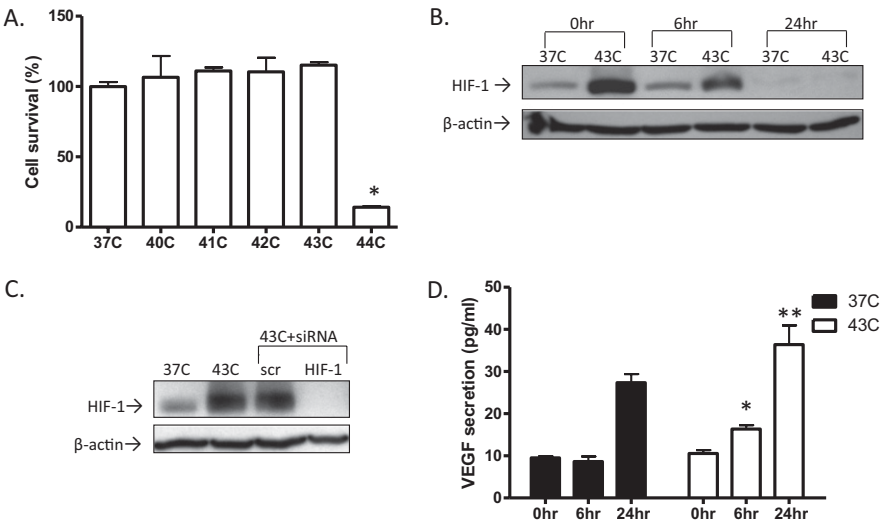

Fig. S1. HT-induced HIF-1 activation in vitro. (*A*) Cytotoxic effects of heat on 4T1 cells were determined by clonogenic assay. After 1 h of HT at temperatures where HIF-1 was activated, cells were further incubated and grown for 7 d until they formed colonies. Colonies containing more than 50 cells were counted and normalized to the control (mean ± SD, $n = 3$, $P < 0.005$). (*B*) A HT-induced increase in HIF-1α protein expression in 4T1 cells was monitored using Western blot. Increased HIF-1α protein levels returned to basal levels at later time points, 6 and 24 h post-treatment. Blots are representative of three independent experiments. (*C*) HIF-1α protein expression was assessed by Western blot after transfecting MDA-MB-231 cells with HIF-1α–specific siRNA. Compared with wild-type MDA-MB-231 cells or with cells transfected with scrambled siRNA, HIF-1α knockdown cells showed decreased HIF-1α expression even after HT. Blots are representative of three independent experiments. (*D*) VEGF secretion into cell media was evaluated in 4T1 cells using ELISA. Compared with the control treatment, HT increased levels of VEGF secretion, and they were statistically significant 6 and 24 h after treatment compared with the control at the same time points (mean ± SD, $n = 3$, $^*P < 0.05$, $^{**}P < 0.005$). Data are representative of three independent experiments.

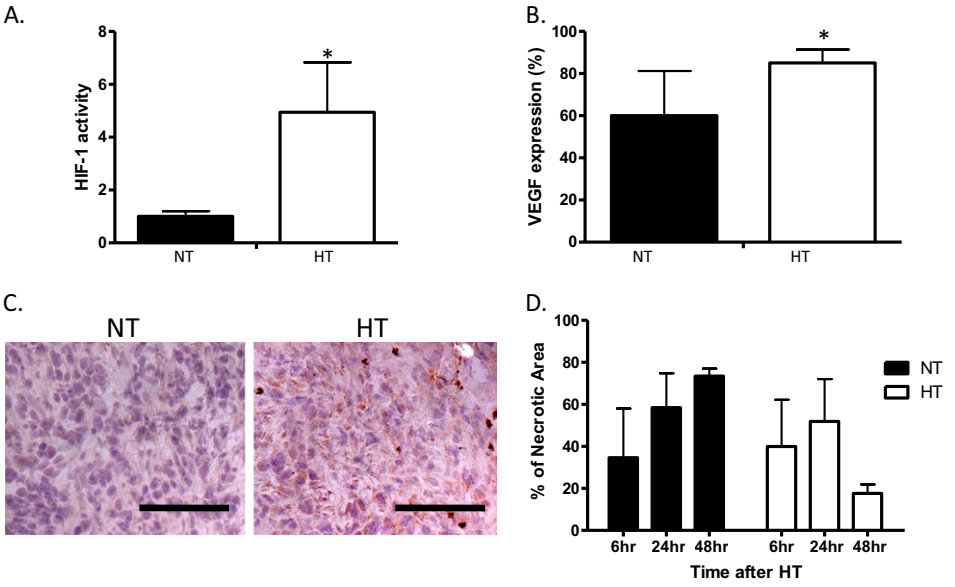

Fig. S2. Increased HIF-1 activity and VEGF expression in mouse tumor tissues after HT. (*A*) HIF-1 activity was evaluated using ELISA in mouse tumor tissues after HT. Consistent with HIF-1α reporter activity, there was a significant increase in HIF-1 activity 6 h after HT (NT: normothermia, HT: hyperthermia; mean ± SEM, $n = 5$, $^*P < 0.05$). (*B* and *C*) VEGF expression in mouse tumor tissues was determined by immunohistochemistry. Forty-eight hours after HT, VEGF-positive tumor tissue areas, represented as brown staining in *C*, were significantly increased (NT: normothermia, HT: hyperthermia; mean ± SEM, $n = 5$, $^*P < 0.05$). (*D*) Using H&E staining, necrotic areas in tumor tissues were determined. Compared with the control, the HT group did not show any significant change in necrotic areas (mean ± SEM, $n = 5$, $P > 0.05$).

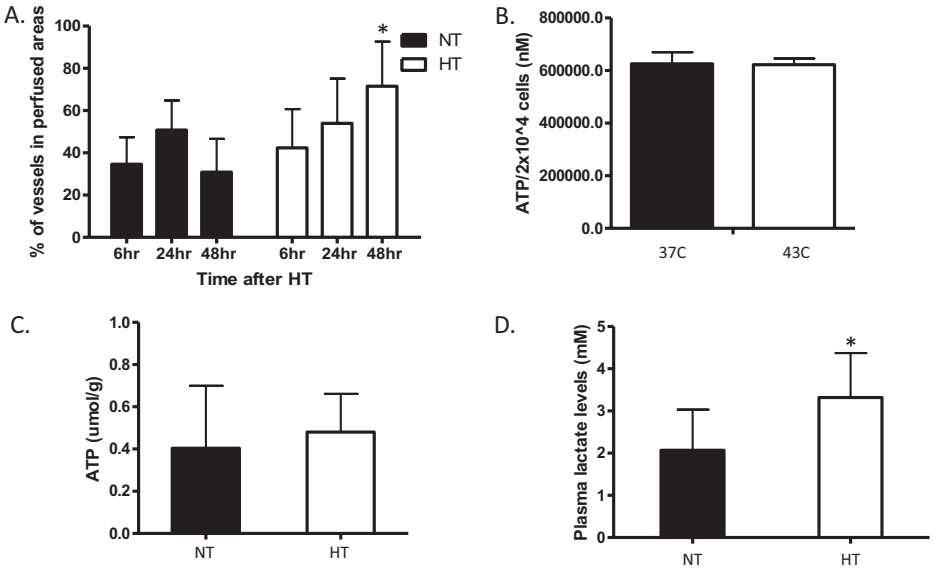

Fig. S3. Increased perfused blood vessel formation with no changes in ATP levels. (*A*) Spatial distribution of tumor blood vessels in perfused areas (Hoechst 33342 positive) was assessed in mouse tumor tissues. Compared with the control, the percentage of blood vessels in perfused areas was significantly increased 48 h after HT (NT: normothermia, HT: hyperthermia; mean ± SEM, $n = 5$, $^*P < 0.05$). (*B*) After HT, tumor cell ATP levels were measured using a CellTiter-Glo Luminescent Cell Viability Assay kit (Promega). HT treatment did not change ATP levels in 4T1 cells (mean ± SD, $n = 3$, $^*P > 0.05$). Data are representative of three independent experiments. (*C*) ATP levels in mouse tissues were measured 6 h after treatment using bioluminescence. Between control and HT groups, there was no significant difference in ATP levels (mean ± SEM, $n = 3$, $P > 0.05$). (*D*) Six hours after HT, lactate levels in mouse plasma were assessed. HT-treated animals showed significantly higher lactate levels than controls (NT: normothermia, HT: hyperthermia; mean ± SEM, $n = 5$, $^*P < 0.05$).

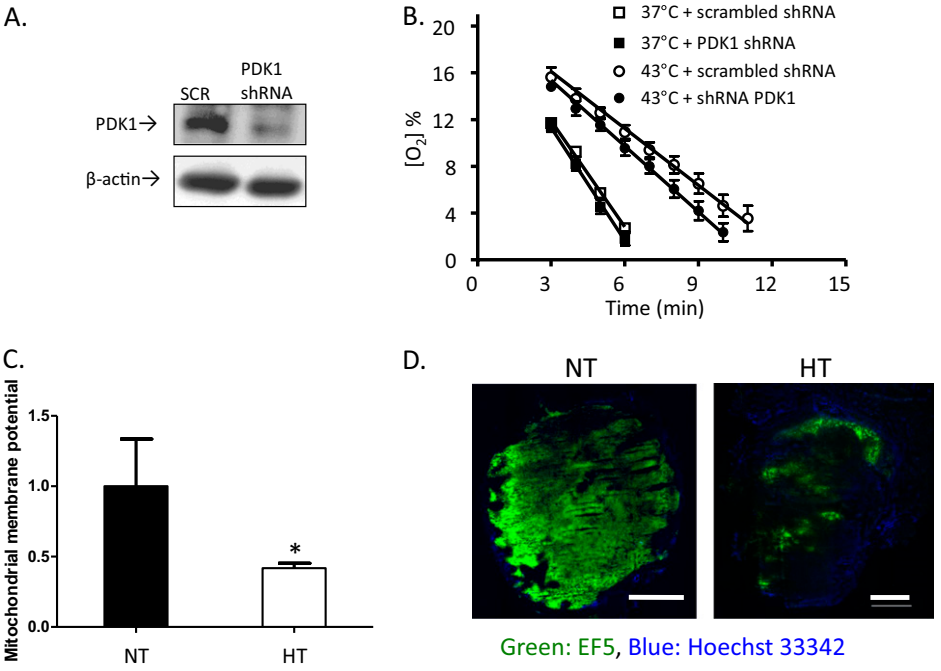

Fig. S4. The role of PDK1 in decreased oxygen consumption rates after HT and a direct effect of HT on mitochondria membrane potential. (*A* and *B*) PDK1 was stably knocked down in 4T1 cells using shRNA. After HT, tumor oxygen consumption rates were determined using EPR oximetry in cells with or without PDK1 knockdown. PDK1 knockdown cells showed a partial blockade of the HT-induced decrease in oxygen consumption rates compared with the control cells transfected with scrambled shRNA (slopes, 37 °C scrambled: −3.031 ± 0.031; 37 °C PDK1 shRNA: −3.223 ± 0.056; 43 °C scrambled: −1.625 ± 0.033; 43 °C PDK1 shRNA: −1.877 ± 0.033, mean ± SD, $n = 8$–9; 37 °C scrambled vs. 43 °C scrambled, $P < 0.0001$; 37 °C scrambled vs. 37 °C PDK1 shRNA, $P < 0.024$; 43 °C scrambled vs. 43 °C PDK1 shRNA, $P < 0.0001$). (*C*) Using the fluorescent dye JC-1, mitochondrial membrane potential was measured to determine mitochondrial function. Compared with the control, HT-treated 4T1 cells showed significantly decreased mitochondrial membrane potential (mean ± SD, $n = 3$, $^*P < 0.05$). Data are representative of three independent experiments. (*D*) Tumor tissues were more hypoxic (EF5: green) and less perfused (Hoechst 33342: blue). Representative images are from tumor tissues excised 24 h after treatment (scale bar: 500 μm).

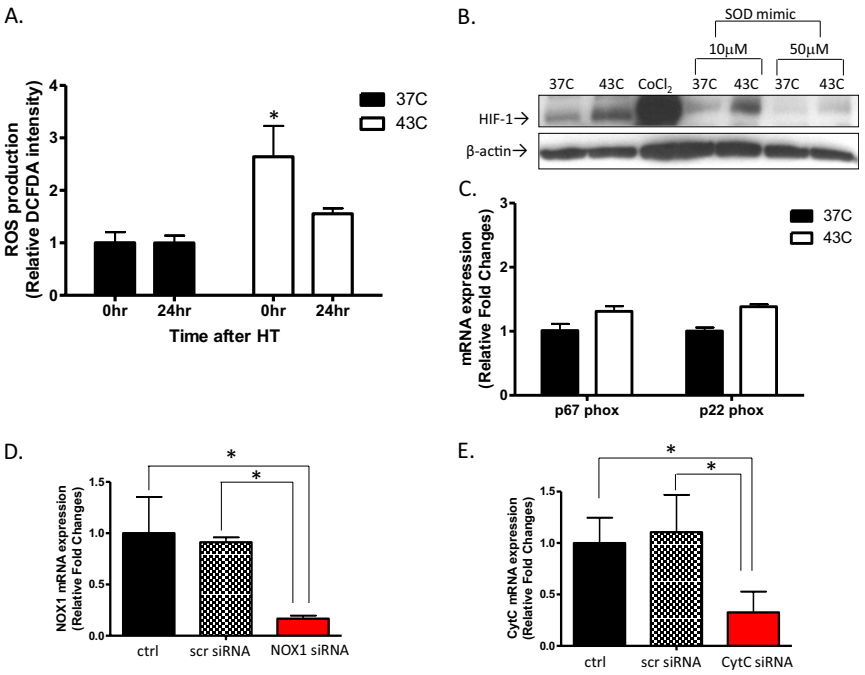

Fig. S5. Effect of HT on ROS production and NADPH oxidase subunits. (*A*) ROS production was measured using CM-H_2DCFDA in 4T1 cells. ROS production was significantly increased immediately after HT (0 h) (mean ± SD, $n = 3$, $^*P < 0.01$) and returned to basal levels within 24 h. Data are representative of three independent experiments. (*B*) To determine the role of ROS in HT-induced HIF-1α up-regulation, 4T1 cells were treated with a manganese (Mn)-porphyrin-based superoxide dismutase (SOD) mimic and peroxynitrite scavenger, Mn(III) *meso*-tetrakis(*N*-ethylpyridinium-2-yl)porphyrin (MnTE-2-PyP^{5+}) (1). With MnSOD mimetics, HIF-1α protein expression was not increased even after HT. Blots are representative of three independent experiments. (*C*) mRNA expression of two other NADPH oxidase subunits, p22phox and p67phox, was determined by qPCR. Compared with the control treatment, there was no significant change in p22phox and p67phox mRNA expression after HT (mean ± SD, $n = 3$, $P > 0.05$). Data were normalized to 37 °C. (*D* and *E*) Transfecting MDA-MB-231 cells with NOX1 (*A*) or cytochrome C (*B*) specific siRNAs significantly decreased their mRNA expression, which was measured by qPCR (mean ± SD, $n = 3$, $^*P < 0.05$).

1. Batinić-Haberle I, Rebouças JS, Spasojević I (2010) Superoxide dismutase mimics: Chemistry, pharmacology, and therapeutic potential. *Antioxid Redox Signal* 13:877–918.

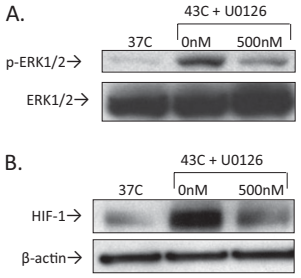

Fig. S6. Regulation of NADPH oxidase through the ERK pathway. (*A*) U0126, an ERK pathway inhibitor, reduced phosphorylated ERK close to basal levels, as shown by Western blot. (*B*) Inhibition of the ERK pathway using 500 nM of U0126 decreased HT-induced HIF-1α protein expression determined by Western blot.

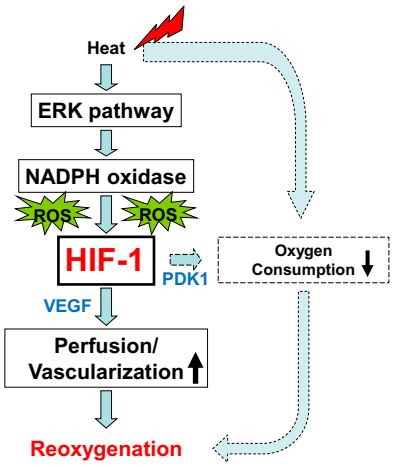

Fig. S7. Diagram of the NADPH oxidase-mediated pathway of HIF-1 activation in tumors after HT. In tumors, HT activates HIF-1 via ERK-NADPH oxidase-ROS pathways. Up-regulation of HIF-1 target genes results in increased tumor perfusion/vascularization and partially decreased oxygen consumption, which results in decreased tumor hypoxia.

Table S1. Primers used for quantitative real-time reverse-transcriptase PCR

Gene	Sequences
Mouse HIF-1α	Forward: 5′-TCTCGGCGAAGCAAAGAGTCTGAA-3′ Reverse: 5′-TAGACCACCGGCATCCAGAAGTTT-3′
Mouse VEGF	Forward: 5′-CTCTCACCGGAAAGACCGATTAAC-3′ Reverse: 5′-GAGTCTCCTCTTCCTTCATGTCAG-3′
Mouse PDK1	Forward: 5′-CAACTACCCTTGGTATGGTATGGG-3′ Reverse: 5′-CGTGGGAGATAAGAAGACCATCTG-3′
Human HIF-1α	Forward: 5′-CAAGAACCTACTGCTAATGCCACC-3′ Reverse: 5′-GTATGTGGGTAGGAGATGGAGATG-3′
Human VEGF-A	Forward: 5′-GAGATGAGCTTCCTACAGCACAAC-3′ Reverse: 5′-CTCCAGGACTTATACCGGGATTTC-3′
Human PDK1	Forward: 5′-CTCAAGTAATCCTTCCACCTCAGC-3′ Reverse: 5′-GGAACATACTGAGACCTCATCTCC-3′
Human NOX1	Forward: 5′-TATGAAGTGGCTGTGCTGGT-3′ Reverse: 5′-GAGGTTGTGGTCTGCACACTG-3′
Human p22phox	Forward: 5′-ACCGCCGTGGTGAAGCT-3′ Reverse: 5′-ACCGAGAGCAGGAGATGCA-3′
Human p67phox	Forward: 5′-CCCTGCAACTACCTTGAACCA-3′ Reverse: 5′-GGACTGCGGAGAGCTTTCC-3′
Human cytochrome C	Forward: 5′-CAAATCTCCATGGTCTCTTTGGGC-3′ Reverse: 5′-TACTCCATCAGTGTATCCTCTCCC-3′
Mouse/human β-actin	Forward: 5′-GATTACTGCTCTGGCTCCTAGC-3′ Reverse: 5′-GACTCATCGTACTCCTGCTTGC-3′